Agricultural and Forest Meteorology 272–273 (2019) 40–54

Contents lists available at ScienceDirect

Agricultural and Forest Meteorology

journal homepage: www.elsevier.com/locate/agrformet

Vertical distributions of chlorophyll and nitrogen and their associations with photosynthesis under drought and rewatering regimes in a maize field

Yibo Li[a,b], He Song[a,b], Li Zhou[c], Zhenzhu Xu[a,*], Guangsheng Zhou[a,c,*]

[a] State Key Laboratory of Vegetation and Environmental Change, Institute of Botany, Chinese Academy of Sciences, Beijing, 100093, China
[b] University of Chinese Academy of Sciences, Beijing, 100049, China
[c] Chinese Academy of Meteorological Sciences, China Meteorological Administration, Beijing, 100081, China

ARTICLE INFO

Keywords:
Chlorophyll
Drought episode
Nitrogen
Rewatering
Vertical distribution
Zea mays L

ABSTRACT

In this study, we characterize the vertical leaf distribution of chlorophyll (Chl) and nitrogen (N) content and their associations with leaf photosynthetic responses in *Zea mays* L. under field watering regimes. We simulated five precipitation patterns, including a drought-rewatering sequence using an electric-powered, rainproof shelter. The results indicate the vertical leaf Chl and N distribution versus the cumulative leaf-area index (LAIc) fit well into a significant quadratic function. The simulated precipitation patterns significantly influenced the parabolic curve trajectory patterns and their parameters. Chlorophyll and N contents had the same trend, with a close and positive relationship. Drought stress followed by rewatering increased the slopes of the linear equations but narrowed the parabolic opening of the quadratic functions. This finding implies that the relationship between Chl and N content can be used to estimate responses to drought and rewatering. The findings also suggested that the relationship patterns between Chl and N levels could be an assessment tool for N-fertilizer managements under different drought conditions to maintain high yields in maize production. Principal component analysis indicated the correlations between functional traits in maize leaves and the responses to drought and rehydration. These findings help to improve drought management and cultivar selection, which will be important in coping with the severe intensity and high frequency of episodic drought events expected from climate change.

1. Introduction

Climate change has caused abnormal changes in precipitation patterns and frequencies (IPCC, 2014; Trenberth et al., 2014; Schwantes et al., 2017), leading to unpredictable water shortages. Water availability is a key factor that limits photosynthetic capacity, plant growth, and grain yield (Boyer, 1982; Li et al., 2006; Guanter et al., 2014; Lobell et al., 2014; Jin et al., 2017; Myers et al., 2017), and many studies have shown that the benefits from elevated CO_2 or increased atmospheric nitrogen (N) deposition induced by climate change will scarcely offset the negative impacts due to abnormal temperature increases and the frequent occurrence of severe drought (Lobell et al., 2014; Gray et al., 2016; Myers et al., 2017). In particular, drought is especially accelerated due to enhanced evaporation in entire ecosystems in response to climate warming; however, the complex responses of crop biological processes and final productivity to climate change need further exploration.

Plants have evolved different adaptive genetic and eco-physiologic strategies, such as enhancements for drought avoidance and tolerance, to deal with environmental changes, such as water-deficit stress (Chaves et al., 2003; Cattivelli et al., 2008). For example, plants enlarge root systems to obtain more water under drought conditions in an adaptive response to soil water deficit stress (Sharp et al., 2004). This root hydrotropic response observed under drought and partial lateral

Abbreviations: A_{sat}, light-saturated photosynthetic rate (μmol m^2 s^{-1}); Chl, chlorophyll content; C_i, intercellular CO_2 concentration (μmol CO_2 mol^{-1}); *E*, transpiration rate (mmol m^{-2} s^{-1}); ETR, Electron transport rate; *Fv/Fm*, maximal efficiency of PSII photochemistry; F_v'/F_m', maximum quantum yield, efficiency of excitation capture by open PSII centers; g_s, stomatal conductance (mol m^{-2} s^{-1}); LAIc, cumulative leaf-area index (m^2 m^{-2}); LRI, leaf-rolling index (%); N_{mass}, nitrogen content based on biomass (mg N g^{-1} dry mass); NPQ (q_N), non-photochemical quenching; PNUE, photosynthetic nitrogen-use efficiency (μmol CO^2 g^{-1} N s^{-1}); PSII, photosystem II, the first protein complex in the light-dependent reactions of oxygenic photosynthesis; q_P, photochemical quenching; SLA, specific leaf area (cm^2 g^{-1} dry mass); SLN, specific leaf nitrogen (g m^{-2}); SPAD, Relative chlorophyll content (a.u.); WUE_a, leaf water-use-efficiency (*Asat*/E, g CO_2 mg^{-1} H_2O); WUE_i, intrinsic water-use-efficiency (*Asat*/g_s); Φ_{PSII}, quantum yield of PSII electron transport

* Corresponding authors.
E-mail addresses: xuzz@ibcas.ac.cn (Z. Xu), gszhou@ibcas.ac.cn (G. Zhou).

https://doi.org/10.1016/j.agrformet.2019.03.026
Received 30 November 2018; Received in revised form 27 March 2019; Accepted 30 March 2019
Available online 07 April 2019

irrigation can improve drought avoidance in maize (*Zea mays* L.) (Eapen et al., 2017). In *Arabidopsis* plants, drought tolerance can be enhanced by the overaccumulation of antioxidant flavonoids (Nakabayashi et al., 2014). These strategies help plants to maintain growth and physiological activities to some degree under adverse conditions (Schulze, 1986; Ruiz-Sánchez et al., 2000; Cattivelli et al., 2008; Xu et al., 2010).

Maize, wheat and rice are the three major staple crops grown for global human consumption, livestock feed and raw materials for industrial purposes (Meng et al., 2013; Zhou et al., 2017; FAO, 2019). To date, drought stress is the main factor limiting maize productivity (Sharp et al., 2003; Zhang et al., 2011) and results in 25–30% reductions in yield in some vulnerable areas (Ben-Ari et al., 2016). However, the responses of maize to precipitation alterations in the field remain poorly understood from the viewpoint of vertical functional distribution, which is defined as changes in patterns of functional traits, such as photosynthetic activity, chlorophyll (Chl), and N content, along the plant height (e.g., Hikosaka et al., 2016). Simultaneous improvements in productivity and water use might be obtained through crop structural modifications (Drewry et al., 2014); thus, vertical functional distribution is an important factor that requires investigation.

Nitrogen content in the canopy shows vertical N distribution. N content is an important parameter that determines the nutritive status of crops, so monitoring N can provide a vital reference for field fertilization management, crop growth performance, and yield estimation (Greenwood et al., 1986; Juh et al., 2011; Ata-Ul-Karim et al., 2017). Many species of plants can regulate their growth and development under field conditions by adapting to the absorbed light profile, which closely correlates with the canopy N distribution and current climate conditions (Chen et al., 2015; Hikosaka et al., 2016). For instance, leaf Chl and N content may show suitable vertical distributions along plant height that match the changes in available radiation (Hirose and Werger, 1987; Escobar-Gutiérrez and Combe, 2012; Hikosaka et al., 2016; Muryono et al., 2017).

The vertical distribution patterns of leaf N are regulated by N redistribution to growth centers/sinks and serve as an adaptive response to the light distribution in the canopy to maximize the canopy photosynthetic rate and total canopy carbon assimilation (Adachi et al., 2017; Walker et al., 2018). Generally, the leaf layers in the upper canopy absorb most of the incoming photosynthetic photon flux density (PPFD); however, the lower layers may still retain high photosynthetic potential (Drewry et al., 2014; Long et al., 2015). Reductions in leaf Chl content in response to reduced canopy light absorption may increase the assimilation efficiency of the vertical light distribution within the canopy (Gu et al., 2017; Walker et al., 2018). In addition, reduced chlorophyll antenna size in the photosystems may also improve photosynthetic solar energy conversion efficiency and finally increase photosynthetic productivity and plant biomass (Kirst et al., 2017). A strong relationship exists between leaf Chl and N content in crops, and this relationship is closely associated with grain yields (Houles et al., 2007; Schlemmer et al., 2013; Parajuli et al., 2018).

In the leaves of vegetable and crop species, 70–80% of the N content is allocated to chloroplasts, which are responsible for photosynthetic activity (Evans, 1983; Sinclair and Horie, 1989; Makino and Osmond, 1991; Mae, 1997; Xu and Zhou, 2006). Thus, although still debated (e.g., Schepers et al., 1992; Blackmer and Schepers, 1995; Dordas, 2017), measuring one parameter (e.g., N) can in theory accurately provide estimates of another (e.g., photosynthesis), depending on the cultivar, environmental conditions, growth stage, and management practices. Leaf Chl and N content often decrease under drought and can thus be taken as proxies of drought stress degree for crop plants (Xu and Zhou, 2006; Arunyanark et al., 2008; Parajuli et al., 2018; Song et al., 2018). Leaf N levels also reflect N availability in the soil (Schröder et al., 2000; Xu and Zhou, 2006). Elucidating the vertical Chl and N distributions and their associations in the responses to alterations in precipitation patterns in a crop field can therefore improve our understanding of the regulatory mechanisms that plants must invoke when faced with continual adverse climatic change (Lobell et al., 2014; Chen et al., 2015; Myers et al., 2017). It is also of importance to improve water and N management in precision farming (Myers et al., 2017; Delloye et al., 2018).

Many researchers have studied the changes in physiological functional traits in different layers within a vertical canopy (e.g., Ciampitti and Vyn, 2013; Chen et al., 2015; Song et al., 2018). In many vegetation types, general exponential functions exhibit a good fit for Chl or N and LAI increases along the plant height (e.g., Hikosaka et al., 2016). However, the vertical distributions of both Chl and N and their associations with photosynthesis within the plant canopy following drought stress and rewatering in the field are unclear.

In the present study, we conducted a field experiment in a large-sized rain-shelter designed to grow maize plants under different irrigation regimes, including drought and subsequent reirrigation. Our study objectives were 1) to examine the vertical distributions of leaf Chl and N within a closed maize canopy and 2) to explore the responses of vertical Chl and N distributions to different watering regimes. Accordingly, we hypothesized that 1) the relationship between the vertical canopy Chl and N changes and the cumulative leaf-area index (LAIc) may show a good fit with conventional exponential functions, thereby indicating a maximization of canopy photosynthesis in maize plants; 2) the relationship between Chl and N content due to their vertical distribution changes could show a good fit with close and positive linear function; and 3) the trajectories of leaf Chl and N distributions along a vertical gradient within the canopy and their relationships would be modified by drought experience. We also considered that the findings would provide a better understanding of the vertical distribution of leaf functional traits and the responses to precipitation/watering regimes, thereby helping to clarify the underlying mechanisms affected by climatic change and to corroborate the theoretical and technological strategies currently in use for drought-resistance management and cultivar breeding.

2. Materials and methods

2.1. Study site description

The experiment was conducted at the Jinzhou Ecology and Agricultural Meteorology Center, Liaoning Province, Northeastern China (N 41°49′, E 121°12′, 27.4 m a.s.l.). This area has a temperate continental monsoon climate with four distinctive seasons. The main crop grown is maize. The mean annual temperature and the mean annual rainfall from 1981 to 2010 were 9.9 °C and 564 mm, respectively, with a mean monthly temperature of 20.9 °C and a total precipitation of 468 mm during the maize growing seasons. The annual frost-free period is 144–180 days. The daily mean air temperature and summed precipitation in the experimental site in both 2015 and 2016 are shown in Fig. S1. The soil is typical brown soil. Representative values of pH, organic matter content, and the soil bulk density were 6.3, 1.8%, and 1.61 $g{\cdot}cm^{-3}$ at 0–100 cm, respectively. The field water content was 22.3%, and the wilting humidity was 6.5%. The mean annual seeding date and maturity date were April 27th and September 16th, respectively (Song et al., 2018).

2.2. Experimental design

The experiment was performed during the two growth seasons in 2015 and 2016 using an electrically powered waterproof shelter (Fig. 1) that is 4 m in height and prevents natural precipitation from falling on the plants under it. When it rains, this system covers the experimental area to exclude natural rainfall. When rain is not falling, it is moved away to make the plots similar to the external field environmental conditions. Each plot is 15 m^2 in area (5 m length, 3 m width) and surrounded by a cement wall raised 0.1 m above the soil surface and

Fig. 1. The experimental plots and powered waterproof shelter shielding maize from natural rainfall, and waterproof shelter with sprinkler system to simulate precipitation patterns in the field. Photos were taken by Yibo Li in 2016.

deeply sunk 1.9 m to prevent water penetration. The experimental plots were surrounded entirely by maize plants, and the entire soil surface was flat. The target precipitation patterns were simulated using a sprinkler irrigation system (Fig. 1). Five watering treatments were established in this experiment for each year: T_1, control; and T_2, water withholding during the jointing-tasseling stage [27 days, 37–64 days after sowing (DAS)]; T_3, the jointing-anthesis stage (41 days, 37–78 DAS); T_4, the tasseling-milking stage (41 days, 51–92 DAS), and T_5, the silking-milking stage (34 days, 58–92 DAS). In this setup, irrigation was supplied at 260, 188, 138, 136, and 161 mm over the entire period of plant development, respectively. The monitored soil relative water content at 0–50 cm soil depth was reduced to the severe drought levels of a range of 30–40% at the end of each rainfall-withholding episode, whereas normal soil water status levels of 70–80% were maintained in the control and postdrought plots after rewatering. Detailed information on the experimental design can be found in our previous report (Song et al., 2018).

2.3. Leaf gas exchange measurements

We measured gas exchange parameters *in situ* using a CIRAS-2 gas exchange system with a Chl fluorescence module (CFM) (PP Systems, Hertfordshire, UK) on mornings with a clear sky (09:30–11:00 a.m.). The leaf chamber reference CO_2 concentration was maintained at 380–390 μmol mol^{-1} with a relative air humidity of 50–70%, and a saturated PPFD of 1500 μmol $m^{-2}s^{-1}$ was used. Gas exchange parameters were obtained at three plant positions (top, middle, bottom), and each position was measured thrice from the middle part of fully developed leaves, avoiding the main veins. The measured parameters included the light-saturated photosynthetic rate (A_{sat}), stomatal conductance (g_s), and transpiration rate (E). Water-use efficiency (WUE) was expressed as A_{sat}/E, and intrinsic water-use efficiency (WUEi) was expressed as A_{sat}/g_s. Leaf Chl fluorescence was also measured simultaneously (see below). Uniform plants were selected in the center of each plot, and each leaf along the vertical plant height was measured. We measured the parameters at the middle zone of the leaf 3–5 times for each watering treatment (Fig. S2).

2.4. Leaf Chl fluorescence measurements

During the plant-growing season in 2015, leaf Chl fluorescence was measured using a portable fluorimeter (Mini-PAM; Walz, Effeltrich, Germany) under dark conditions at night (21:00–23:00 p.m.). Following at least 2 h of dark adaptation, the minimal fluorescence yield (F_o) was measured with a modulated light of less than 0.1 μmol photon $m^{-2}s^{-1}$ that would not induce any significant variable fluorescence, and the maximal fluorescence yield (F_m) was obtained with a 0.8-s saturating pulse at 7000 μmol photons $m^{-2}s^{-1}$ in the dark-adapted leaves. In 2016, leaf Chl fluorescence was measured using a CIRAS-2 gas exchange system with a Chl fluorescence module (CFM). Leaves were then light adapted at a light intensity of 1500 μmol m^{-2} s^{-1} for 15 min to measure the steady-state fluorescence (F_s) and then subject to a flash (5100 μmol m^{-2} s^{-1}, with a pulse time of 0.3 s) to measure the maximum fluorescence (F_m'). Then, the leaves were exposed to far-red light for 5 s to determine the minimum light fluorescence (F_o'). We calculated the following Chl fluorescence parameters: the maximal efficiency of photosystem II (PSII) photochemistry (F_v/F_m), maximum quantum yield of PSII photochemistry (F_v'/F_m'), quantum yield of PSII electron transport (Φ_{PSII}), photochemical quenching (q_P), non-photochemical quenching (q_N, NPQ), and electron transport rate (ETR) (Genty et al., 1989; Maxwell and Johnson, 2000; Kramer et al., 2004). These calculations were performed using the following equations:

$$F_v/F_m = (F_m\text{-}F_o)/F_m$$

$$F_v'/F_m' = (F_m'\text{-}F_o')/F_m'$$

$$\Phi_{PSII} = (F_m'\text{-}F_s)/F_m'$$

$$q_P = (F_m'\text{-}F_s)/(F_m'\text{-}F_o')$$

$$q_N = (F_m\text{-}F_m')/(F_m\text{-}F_o')$$

$$NPQ = (F_m\text{-}F_m')/F_m'$$

$$ETR = \Phi_{PSII} \times fI\alpha_{leaf}$$

where f is the fraction of the absorbed quanta used by PSII and is typically assumed to be 0.4 for a C_4, a factor that accounts for the partitioning of energy between PSII and PSI (Edwards and Baker, 1993; Maxwell and Johnson, 2000); I is incident PPFD; and α_{leaf} is the leaf absorbance estimated by the relative chlorophyll content determined with the SPAD-502 chlorophyll meter (Minolta Camera Co. Ltd. Japan) based on a function described by Earl and Tollenaar (1997):

$$\alpha_{leaf} = 0.409 + 0.528*(1 - e^{-0.0429*SPAD})$$

2.5. Chlorophyll measurements

The SPAD-502 chlorophyll meter was used to determine the relative Chl content (recorded as "SPAD" readings, a.u.) for each leaf. Every leaf was measured 4–6 times per sampling occasion, avoiding the leaf midrib, and the mean values were determined for each watering regime. The total SPAD value per plant, a value weighted by leaf area, was calculated as follows:

$$Total\ Chl\ content\ /\ plant = \sum_{i}^{n} Area\ of\ the\ leaf_i \times SPAD\ of\ the\ leaf_i$$

where i is the leaf number from the top to the bottom of the plant, and n is the total number of leaves on the plants. The leaf area is expressed in units of m^2.

2.6. Plant morphometry measurements

The plant height (H, m) and the maximum length (L, cm), real width (W, cm), and natural width (w, cm) of each leaf were measured using the following formula to calculate the leaf area (cm^2), total plant leaf area (cm^2), and leaf-rolling index (LRI, %) (Francis et al., 1969; Xiang et al., 2012):

$$Leafarea = 0.75 \times L \times W$$

$$Totalleafarea = \sum_{i=1}^{n} (0.75 \times L_i \times W_i)$$

$$Leafrollingindex = (W - w)/W$$

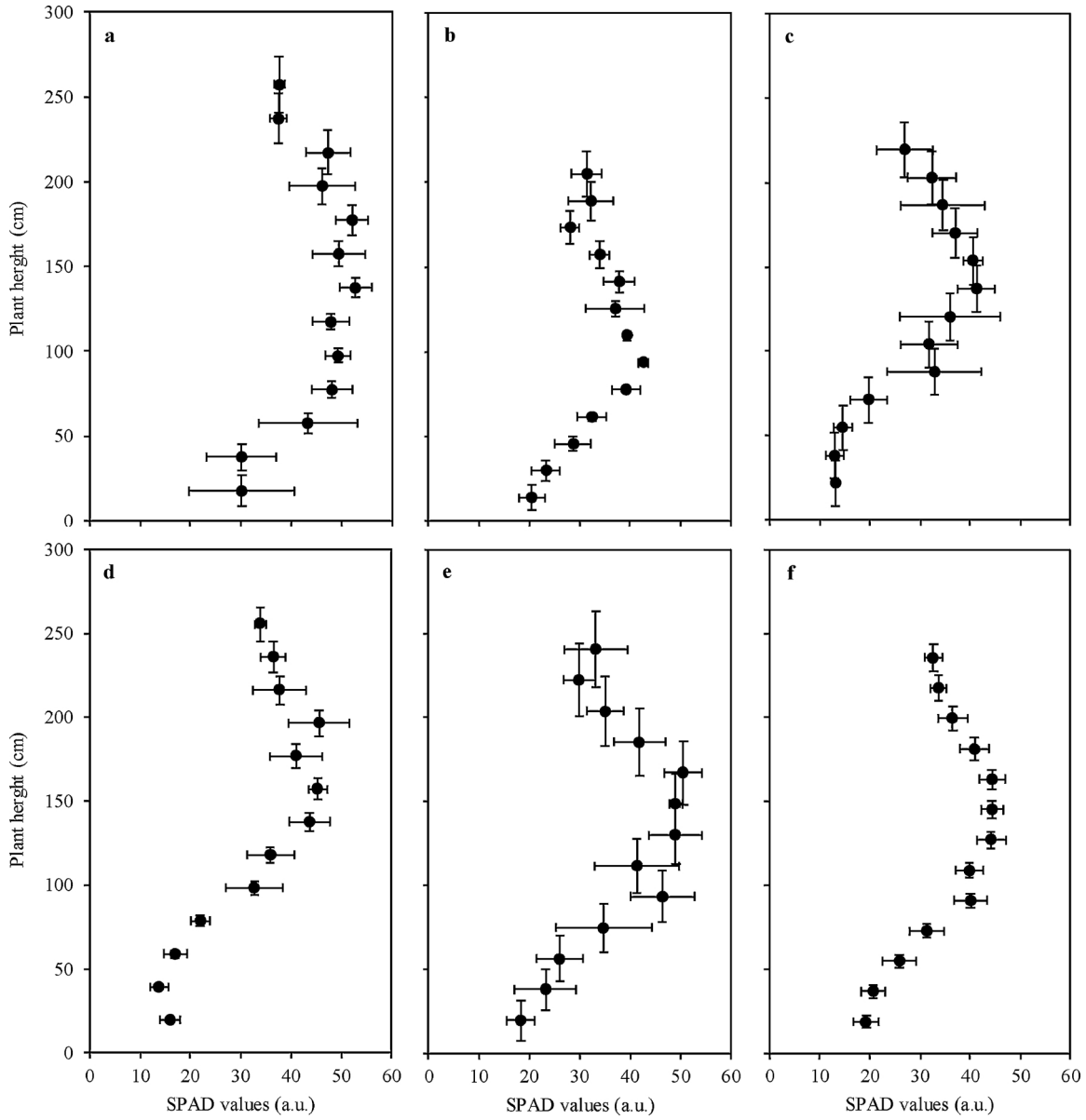

Fig. 2. Canopy vertical distribution of chlorophyll content (SPAD a.u.) under various watering regimes. **a**: T_1, control, normal irrigation; **b**: T_2, withholding water during jointing-tasseling; **c**: T_3, jointing-anthesis; **c**: T_4, tasseling-milking; **e**: T_5, silking-milking. They received 260, 188, 138, 136, and 161 mm of total irrigation during the whole plant growth period, respectively. **f:** Across all watering treatments (n = 3 for panels a–e; n = 15 for panel f).

where L_i and W_i are i-th leaf length and width, respectively. LAIc is the cumulative leaf-area index from the canopy top to the bottom. We measured the area of each leaf from the top to the bottom of the plant and the number of leaves and expressed this per unit ground surface area. We then added the leaf area with increasing leaf number. For example, if $LAIc_1$ = the area of the top leaf × D, then the $LAIc_2$ = (the area of top leaf + the area of the second leaf) × D (Fig. S2). Thus, the final LAIc from the top leaf to the bottom leaf along the plant height is the conventional LAI parameter in a crop field.

$$LAI_C = \sum_{i}^{n} Area\ of\ the\ leaf_i \times D$$

where D is the plant density (plants m^{-2}).

2.7. Nitrogen content measurements

Following the gas exchange and morphological measurements, all leaves were detached, dried at 80 °C to a constant weight in an oven, and then ground with a ball mill (NM200; Retsch, Haan, Germany). The N concentrations (mg N g^{-1} dry mass) in each leaf sample were determined by a modified Kjeldahl method. Specific leaf area (SLA; cm^2 g^{-1} dry mass) was calculated as each leaf area (cm^2) divided by the leaf dry weight (g^-), and the specific leaf N (SLN; g m^{-2}, lea surface area) was calculated as N content (g) per dry weight and whole-leaf area (m^2). The photosynthetic N-use efficiency (PNUE; μmol CO_2 g^{-1} N s^{-1}) was calculated as $A_{sat}/SLN^{-1\ N\ s-}$ (Sinclair and Horie, 1989; Chen et al., 2015). Every leaf from top to bottom was included in this analysis.

2.8. Statistical analyses

Statistical analysis was conducted using SPSS version 20.0 software (SPSS Inc. Chicago, IL). The differences in functional traits among watering treatments, which were determined with a Duncan's multiple comparison test, were tested by ANOVA. The relationships among leaf Chl content, N content, and the LAIc were made using linear and/or nonlinear regression function estimations. The relationships among leaf

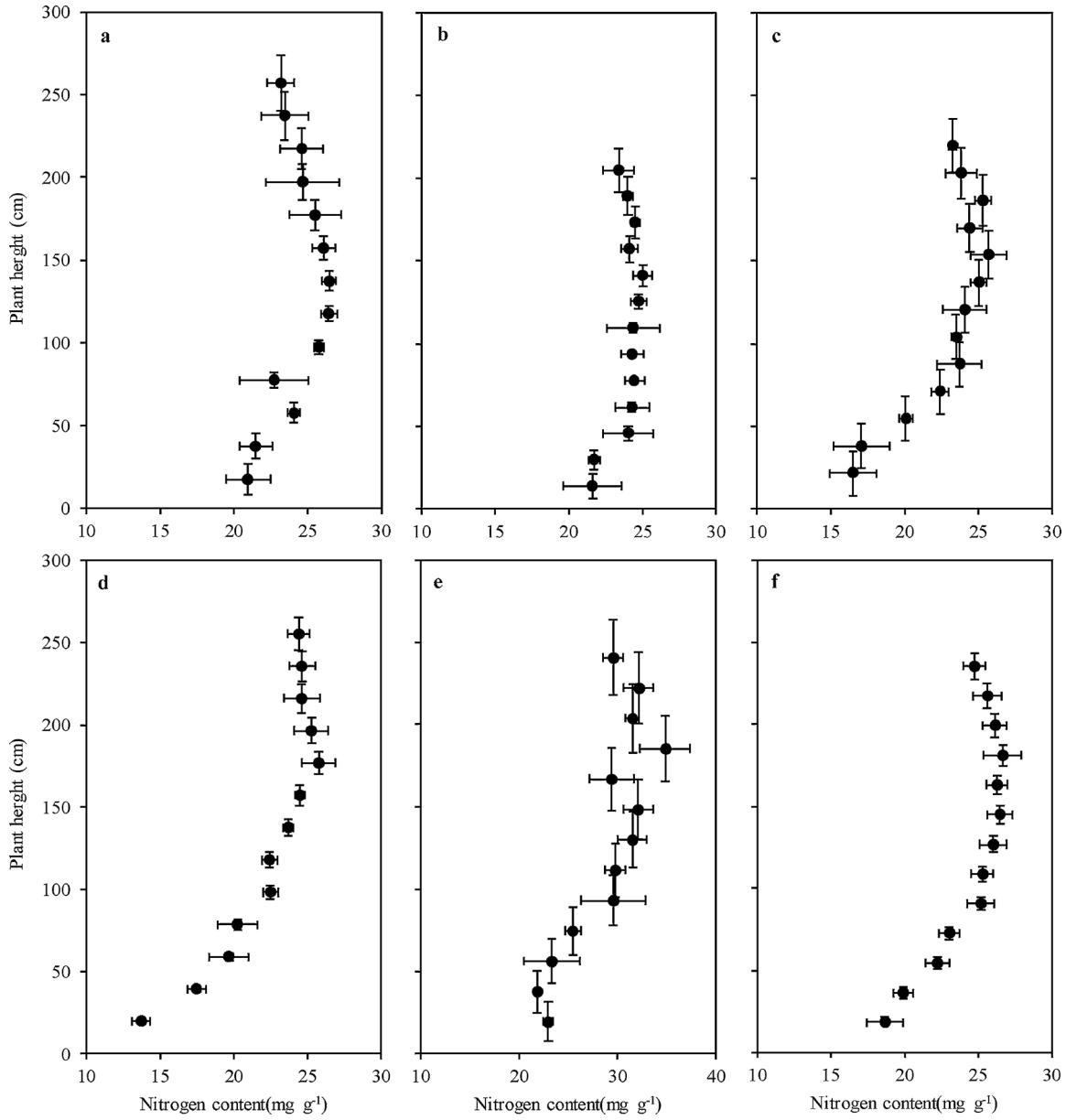

Fig. 3. Canopy vertical distribution of nitrogen content under various watering regimes. **a**: T_1, control, normal irrigation; **b**: T_2, withholding water during jointing-tasseling; **c**: T_3, jointing-anthesis; **c**: T_4, tasseling-milking; **e**: T_5, silking-milking. They received 260, 188, 138, 136, and 161 mm total irrigation during the whole plant growth period, respectively. **f:** Across all the watering treatments (n = 3 for panels a–e; n = 15 for panel f).

Chl content, leaf N content, photosynthetic potentials, morphological traits, and the responses to different watering regimes and canopy layers were tested using principal component analysis (PCA). The significance was set at $P < 0.05$ unless stated otherwise.

3. Results

3.1. Chlorophyll vertical distribution under watering regimes

As shown in Fig. 2, the relationship between the relative leaf chlorophyll content (Chl) and plant height (H) within the maize canopy was unimodal (i.e., hump-shaped). Leaves (often the ear leaf and the leaves above and below the ear leaf) at the central plant height often had the highest Chl content, and Chl levels then decreased above and below these leaves. Watering treatments markedly affected Chl patterns. In the control treatment (T_1, normal irrigation), the highest values were observed in the middle layer at a plant height of 1.4–1.8 m, and the values slowly decreased with increasing height, with the lowest values observed below a height of 0.4 m (Fig. 2a). In the T_2 treatment (withholding water during the jointing-tasseling stage, Fig. 2b), the maximum SPAD value occurred in the lower middle leaves at a height of 0.95 m and decreased at higher or lower height levels, with significant reductions occurring at a height of 0.45 cm and below. The middle leaves in the T_3 condition at a range of 1.2–1.5 m height had greater SPAD values that decreased linearly and sharply as plant height decreased (Fig. 2c). When the drought episode occurred during tasseling-milking (T_4 treatment), Chl levels were highest in the upper-middle leaves, with a linear decrease occurring below a height of 1.4 m (Fig. 2d). Under the T_5 treatment (drought during silking-milking), the highest value was also found in the middle layer and sharply decreased with increasing and decreasing height (Fig. 2e). Over all the watering treatments, the highest Chl levels were observed in middle layer leaves at the middle canopy profile (height of 1.3–1.6 m), which is usually defined as containing the ear leaves (i.e., the ear leaf and the two leaves

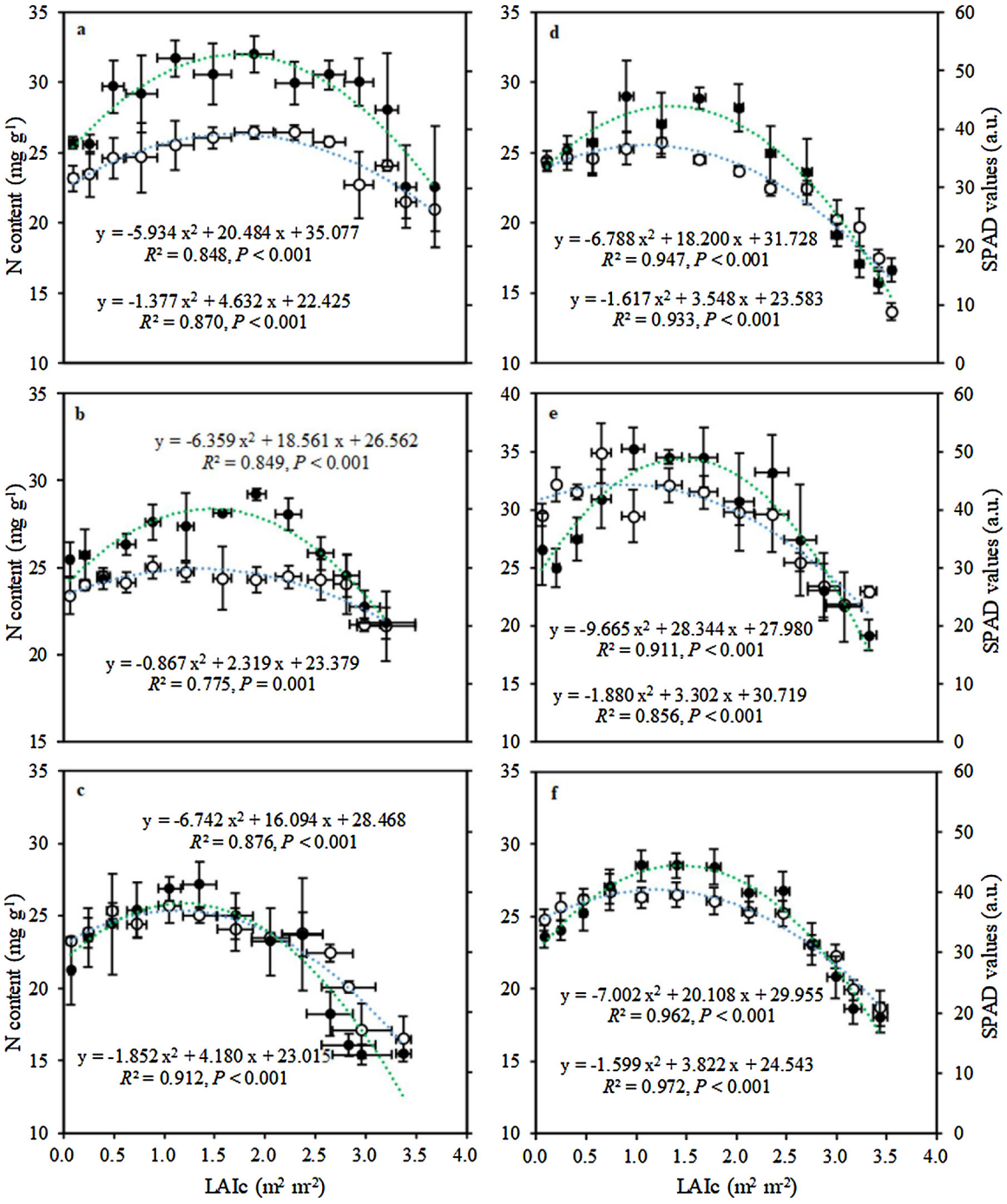

Fig. 4. Vertical changes in chlorophyll and nitrogen content with cumulative leaf-area index (LAIc) under various watering regimes. **a**: T_1, control, normal irrigation; **b**: T_2, withholding water during jointing-tasseling; **c**: T_3, jointing-anthesis; **c**: T_4, tasseling-milking; **e**: T_5, silking-milking. They received 260, 188, 138, 136, and 161 mm total irrigation amount during whole plant growth period, respectively. **f:** Across all the watering treatments (n = 3 for panels a–e; n = 15 for panel f). Closed circles and green dotted lines represent relative chlorophyll content (*i.e.* SPAD values); Open circles and blue dotted lines represent nitrogen content (N_{mass}, mg g^{-1}). The function equations above and below in each panel represent the relationships of chlorophyll and nitrogen content with LAIc, respectively (For interpretation of the references to colour in this figure legend, the reader is referred to the web version of this article).

above and below it) (Fig. 2f). This relationship showed a very good fit to a quadratic function (Chl = -0.002H^2 + 0.480H + 7.450, R^2 = 0.937, P < 0.001).

3.2. Nitrogen vertical distributions under watering regimes

Fig. 3 shows the changes in vertical N patterns within the maize canopy along the canopy height gradient from the top to the bottom in the responses to drought stress followed by rewatering. The observed curves were generally unimodal. Under the control condition (Fig. 3a), the leaves at the middle plant height of 1.4 m contained the highest N content followed by leaves above or below. The change in vertical N distribution under the T_2 treatment was relatively flat when measured at different plant heights. However, exposure to a drought episode during the jointing to anthesis stage (T_3, Fig. 3c) resulted in a gradual decline in N content at heights less than 1.5 m with significant drops below a height of 0.55 m. For the T_4 treatment, in which the drought occurred during the tasseling-milking stage (Fig. 3d), a significant

Table 1
Two quadratic function curves of chlorophyll content (SPAD a.u.) and nitrogen content (N) with the cumulative leaf-area index (LAIc) of maize canopy under different drought conditions (From Fig. 4).

Treatments	Traits	LAI_{cy}	Y_{max}	*a*	*b*	*c*	R^2	*P*
T_1	SPAD	1.73	52.75	−5.934	20.484	35.077	0.85	$P < 0.001$
	N	1.68	26.32	−1.377	4.632	22.425	0.87	$P < 0.001$
T_2	SPAD	1.46	40.11	−6.359	18.561	26.562	0.85	$P < 0.001$
	N	1.34	24.93	−0.867	2.319	23.379	0.78	$P = 0.001$
T_3	SPAD	1.19	38.07	−6.742	16.094	28.468	0.88	$P < 0.001$
	N	1.13	25.37	−1.852	4.180	23.015	0.91	$P < 0.001$
T_4	SPAD	1.34	43.93	−6.788	18.200	31.728	0.95	$P < 0.001$
	N	1.10	25.53	−1.617	3.548	23.583	0.93	$P < 0.001$
T_5	SPAD	1.47	48.78	−9.655	28.344	27.980	0.91	$P < 0.001$
	N	0.88	32.17	−1.880	3.302	30.719	0.86	$P < 0.001$
Total	SPAD	1.44	44.39	−7.002	20.108	29.955	0.96	$P < 0.001$
	N	1.20	26.83	−1.599	3.822	24.543	0.97	$P < 0.001$

Notes: $y = ax^2 + bx + c$; where a, b, and c are constants; R^2 is coefficient of determination; *P* value determines statistical significance. Where the LAIc reached (-b/2a) (LAI_{cy}), the maximum values of the chlorophyll or N content were $(4ac\text{-}b^2)/4a$ ($Ymax$). T_1, T_2, T_3, T_4, and T_5 denote control and withholding water during jointing-tasseling, jointing-anthesis, tasseling-milking, and silking-milking, with 260, 188, 138, 136, and 161 mm of irrigation in the entire plant development, respectively.

change was observed along the vertical height gradient with a steep incline occurring below a height of 1.6 m. The change in vertical N patterns under the T_5 treatment (in which the maize plants were subjected to drought conditions during silking-milking) demonstrated a different profile: the highest N level occurred at an increased height of 1.85 m, and a significant reduction appeared at a height of 1.10 m (Fig. 3e). Across the watering treatments (Fig. 3f), the leaves at a height of approximately 1.8 m showed higher N levels, with significant decreases observed at heights less than 1.1 m. This relationship also showed a good fit with a quadratic function ($Chl = -0.0004H^2 + 0.125H + 16.297$, $R^2 = 0.987$, $P < 0.001$).

3.3. Vertical profile of functional traits with LAIc under watering regimes

Comparing LAIc estimates from the maize plant canopy top against the changes in Chl or N content revealed a good fit with a quadratic function rather than an exponential function or linear function under various watering regimes ($R^2 > 0.75$, $P < 0.01$, Fig. 4a–f). The curve trajectory patterns and parameters, however, were markedly affected by the simulated precipitation regimes (Fig. 4; Table 1).

The analysis of the quadratic functions (Table 1) revealed that the LAIc values for the N maximum were lower than those for the Chl maximum. These findings indicate that high N was distributed in the upper canopy, while low Chl was distributed more extensively in the lower canopy. Across all treatments, the LAIc value was 1.44 m m^{-2} where the Chl content reached its maximum (a SPAD value of 44.39), while LAIc was 1.20 m m^{-2} where N content reached its maximum (a N_{mass} value of 26.83 mg g^{-1}, Table 1). Different simulated precipitation patterns affected these relationships. Compared with control treatment (T_1), the T_2, T_3, T_4, and T_5 treatments resulted in marked decreases of 23.98, 27.83, 16.73, and 7.53%, respectively, in the maximal Chl content along the vertical gradient within the maize plant canopy with a mean reduction of 15.85% (Fig. 4a–f; Table 1). Comparing the N distribution responses to variations in the watering regime revealed that the T_2, T_3, and T_4 treatments reduced the maximal N content along the vertical gradient within the plant canopy by 5.28, 3.60, and 3.01%, respectively. However, the T_5 treatment increased the maximal N content by 22.22%. An average increase of 1.92% was obtained for the maximal N across all 4 drought treatments compared with the control treatment.

A repeat of the same experiment conducted in 2015 revealed similar quadratic function relationships between Chl and F_v/F_m and LAIc for each watering regime (Fig. 5a-j). However, the associations between Chl and LAIc were stronger than those between F_v/F_m and LAIc. Across all watering treatments, the relationships became stronger for both measurement years (Fig. 4f, Fig. 6). The quadratic function curves were modified by the rewatering regimes and showed reductions in the maxima of Chl and F_v/F_m along the LAIc gradient under severe episodic drought, although F_v/F_m remained relatively stable (Figs. 5–6).

3.4. Mean leaf and entire canopy Chl and N content under watering regimes

As shown in Fig. 7, changes in watering treatments significantly affected the mean leaf Chl content (Fig. 7a; $F = 8.91$, $P < 0.001$). A multiple comparison test indicated that drought and subsequent rewatering treatments led to significant declines in Chl content. The lowest value was observed under the T_3 treatment, in which the drought episode occurred during jointing-anthesis. The changes in the amount of Chl in the entire canopy showed a similar trend to the changes in the mean leaf Chl content, but the effects of watering regimes were not statistically significant (Fig. 7b). The mean N content at the leaf scale was significantly affected by the watering regime (Fig. 7c; $F = 24.53$, $P < 0.001$). The greatest leaf N content was observed under the T_5 treatment, and the lowest leaf N content was observed under the T_4 treatment. The different watering regimes did not significantly affect the total amount of N in the entire canopy (Fig. 7d). The highest N value occurred under the control treatment and subsequently decreased with T_5, T_4, T_2, and T_3 treatments.

3.5. Relationships between Chl and N content under watering regimes

The relationships between the changes in Chl and N content along the vertical canopy gradient were analyzed for the different watering treatments. Generally, the relationships of both the linear and quadratic functions appeared to be statistically significant; the quadratic function had a particularly stronger relationship (Fig. 8a–f). The different watering regimes markedly affected these relationships. Specifically, stronger associations between N with Chl were observed with T_3 treatment (linear: $R^2 = 0.85$, $P < 0.001$; quadratic: $R^2 = 0.91$, $P < 0.001$, Fig. 8c), while relatively weaker relationships were noted for T_5 treatment (linear: $R^2 = 0.49$, $P = 0.008$; quadratic: $R^2 = 0.61$, $P = 0.009$, Fig. 8e). A reanalysis of the trajectory patterns for the parabolic curves also showed that episodic drought narrowed the downward opening of the parabola (i.e., drought increased the absolute value of the coefficient *a* of the quadratic function). Across all the watering regimes, the relationships became stronger, as indicated by higher coefficients of determination and significance levels ($R^2 = 0.87$, $P < 0.001$ for the linear equation; $R^2 = 0.95$, $P < 0.001$ for the quadratic function, Fig. 8f). Additionally, the use of all the data (Fig. 9) resulted in better relationships for the linear and quadratic functions: $y = 0.237x$

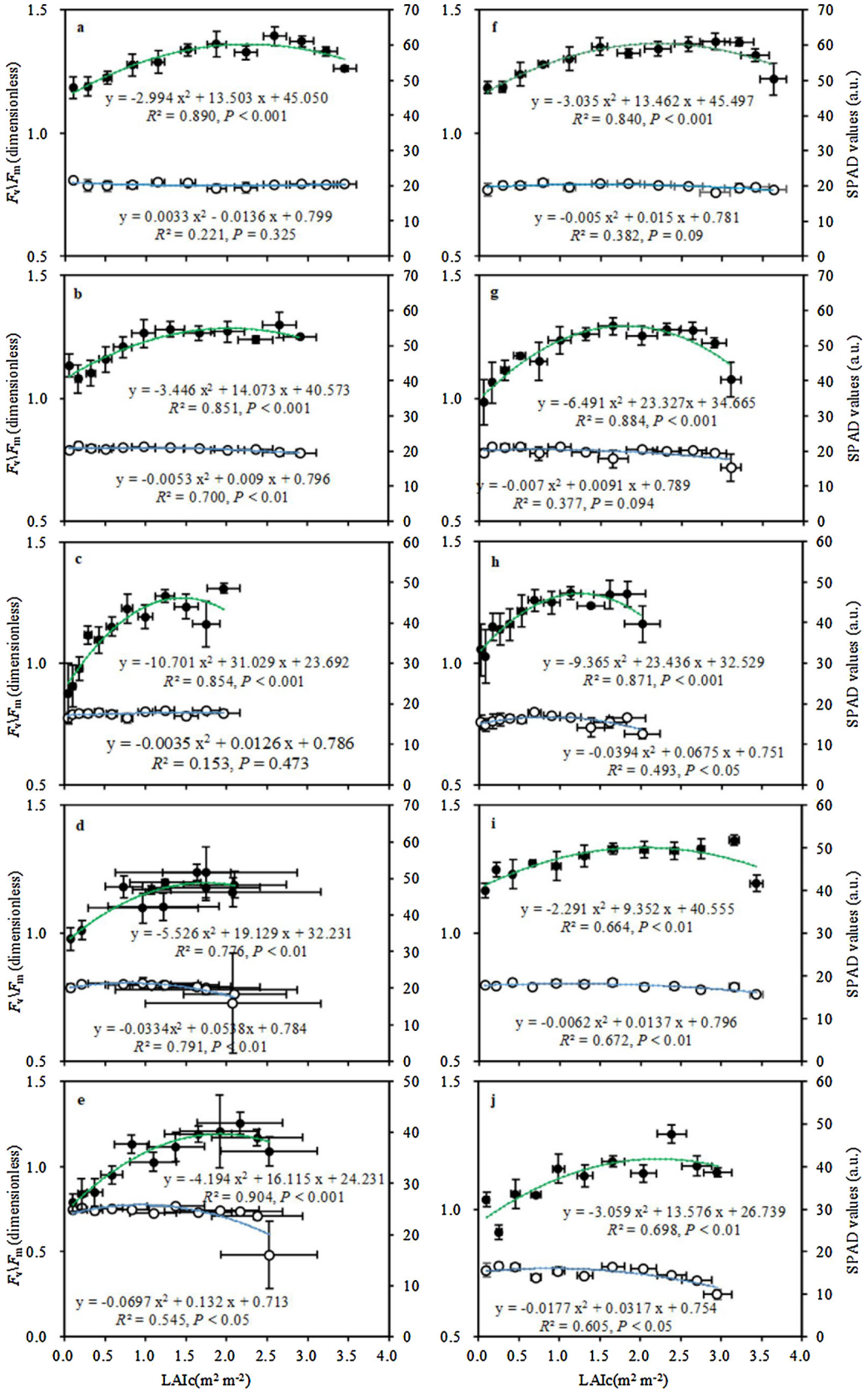

Fig. 5. Associations of chlorophyll content (SPAD a.u.) and maximal efficiency of PSII photochemistry (F_v/F_m, dimensionless) with LAIc under various watering regimes. Measured on 5 (a–e), and 9 (f–j) August, 2015. **a, f**: T_1, control, normal irrigation; **b, g**: T_2, withholding water during jointing-tasseling; **c, h**: T_3, jointing-anthesis; **d, i**: T_4, anthesis-blistering; **e, j**: T_5, anthesis-milking. They obtained 296, 246, 221, 246, and 221 mm total irrigation during the whole plant growth period, respectively, during the 2015 growing season. Closed circles and green dotted lines represent relative chlorophyll content; while open circle and blue dotted line represent F_v/F_m (dimensionless). The function equations above and below in each panel represent the relationships of chlorophyll and nitrogen content with LAIc, respectively ($n = 3$) (For interpretation of the references to colour in this figure legend, the reader is referred to the web version of this article).

+ 16.084 ($R^2 = 0.47$, $P < 0.001$) and y = -0.006 x^2 + 0.646 x + 9.998 ($R^2 = 0.52$, $P < 0.001$). These results demonstrated that the quadratic function was more suitable for fitting the relationship between Chl and N concentrations in crops in response to different watering regimes.

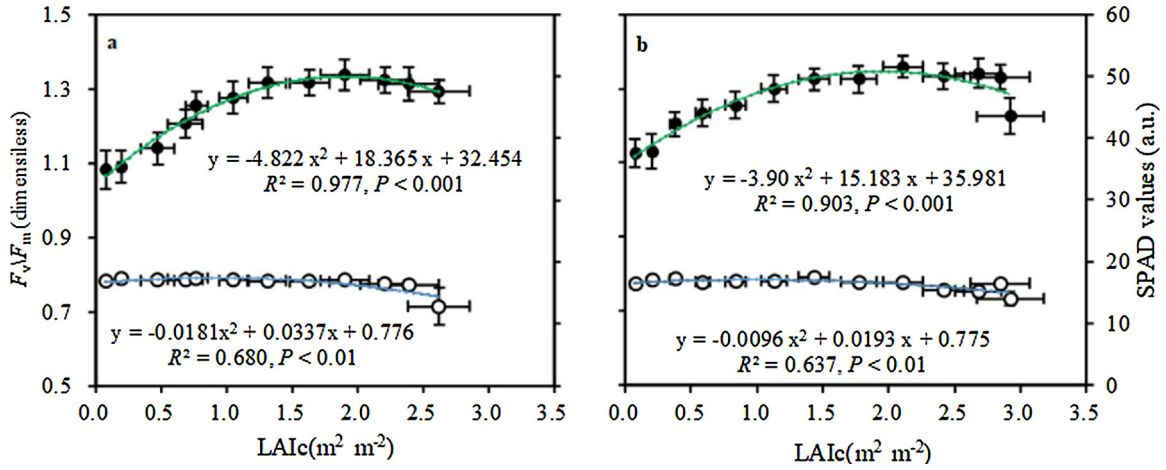

Fig. 6. Associations of chlorophyll content (SPAD a.u.) and maximal efficiency of PSII photochemistry (F_v/F_m) with LAIc across all watering treatments. Measured on 5 (a) and 9 (b) August, 2015. For others, see Fig. 5.

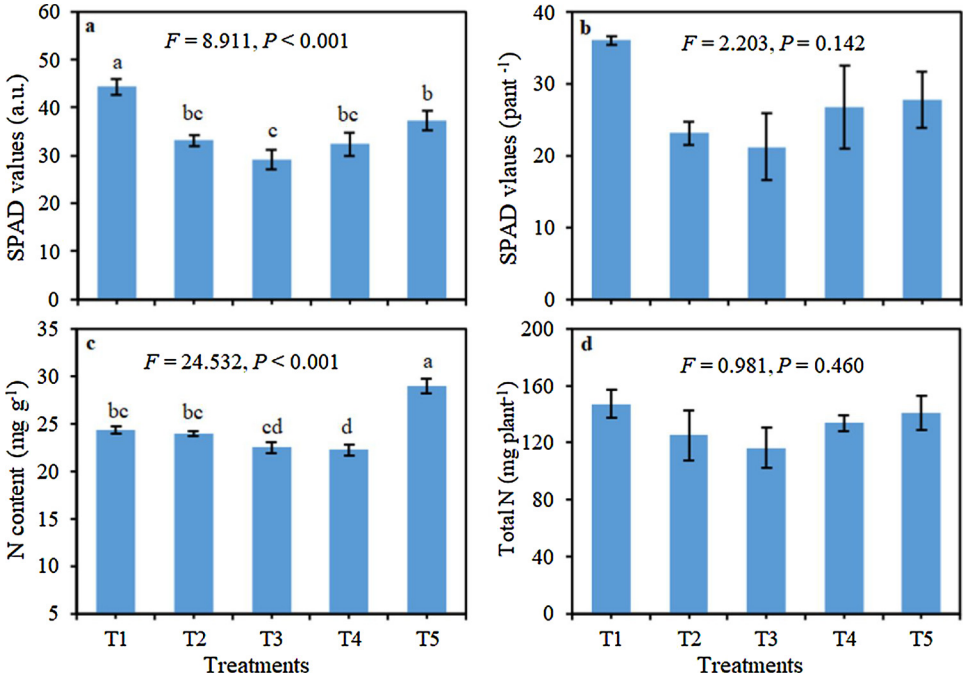

Fig. 7. Mean or total chlorophyll (SPAD a.u.) and nitrogen (N) content at leaf and entire-canopy scales under watering regimes. **a**: mean leaf Chl content; **b**: Chl amount of entire canopy; **c**: mean leaf N content; **d**: Total N amount. T_1, control, normal irrigation; T_2, withholding water during jointing-tasseling; T_3, jointing-anthesis; T_4, tasseling-milking; T_5, silking-milking. They received 260, 188, 138, 136, and 161 mm total irrigation during the whole plant growth period, respectively. Different lowercase letters on the bars indicate significant differences between watering regimes at $P < 0.05$ according to Duncan' multiple comparison test (mean data ± SE; n = 3–5).

3.6. Relationships among multiple functional traits under watering regimes

As shown in Fig. 10, significant relationships appeared between Chl content and light-saturated photosynthetic rate (A_{sat}, $R^2 = 0.39$, $P < 0.001$; Fig. 10a), water use efficiency (WUE, $R^2 = 0.42$, $P < 0.001$; Fig. 10b), and photosynthetic N-use efficiency (PNUE; $R^2 = 0.36$, $P < 0.001$; Fig. 10c). However, only WUE was correlated with N content ($R^2 < 0.20$; Fig. 10d–f). Correlation coefficients between the functional and morphological traits and grain yield are shown in supplementary Table S1. Positive relationships for grain yield with A_{sat} ($R = 0.61$, $P < 0.05$) and leaf Chl content ($R = 0.37$) were observed, but negative relationships with Φ_{PSII} ($R = -0.60$, $P < 0.05$) and N content ($R = -0.33$) were noted.

The PCA conducted on leaf Chl and N content, gas exchanges, and fluorescence traits revealed that the first principal component (PC1) and the second PC2 accounted for 58.4% and 20.8% of the total variations in the functional traits (Fig. 11a), respectively, summing to 79.2% in total. This finding indicated that the first two PCs, particularly PC1, represented the main integrated changes in all the variables. Positive correlations were also observed between PC1 and SPAD, N_{mass}, A_{sat}, g_s, (E), WUE_a(A_{sat}/E), WUE_i(A_{sat}/g_s), and PNUE, and negative correlations were observed between PC1 and C_i, F_v'/F_m', Φ_{PSII}, q_P, ETR, and LRI (a plant structural trait). These findings indicated that PC1 represented most of the gas exchange and Chl fluorescence parameters. Negative relationships were observed between PC2 and q_N, and NPQ. The location of LRI was the inverse of the patterns observed for the changes in g_s and carbon-fixation capacity. The SLA showed a weak positive correlation with both PC1 and PC2 but a strong correlation with PC3 ($R = -0.76$). The distribution patterns of the factor scores demonstrated that the factors under control treatment and those in the upper and middle leaves were mostly located in the right part of the graph, while those that experienced severe drought and located in the bottom leaves were mostly located in the left part (Fig. 11b).

4. Discussion

Many studies on field-grown maize have reported high levels of functional traits related to photosynthetic capacity in the middle canopy leaves after silking (Dwyer and Stewart, 1986; Escobar-Gutiérrez and Combe, 2012; Song et al., 2018). The present results also indicated

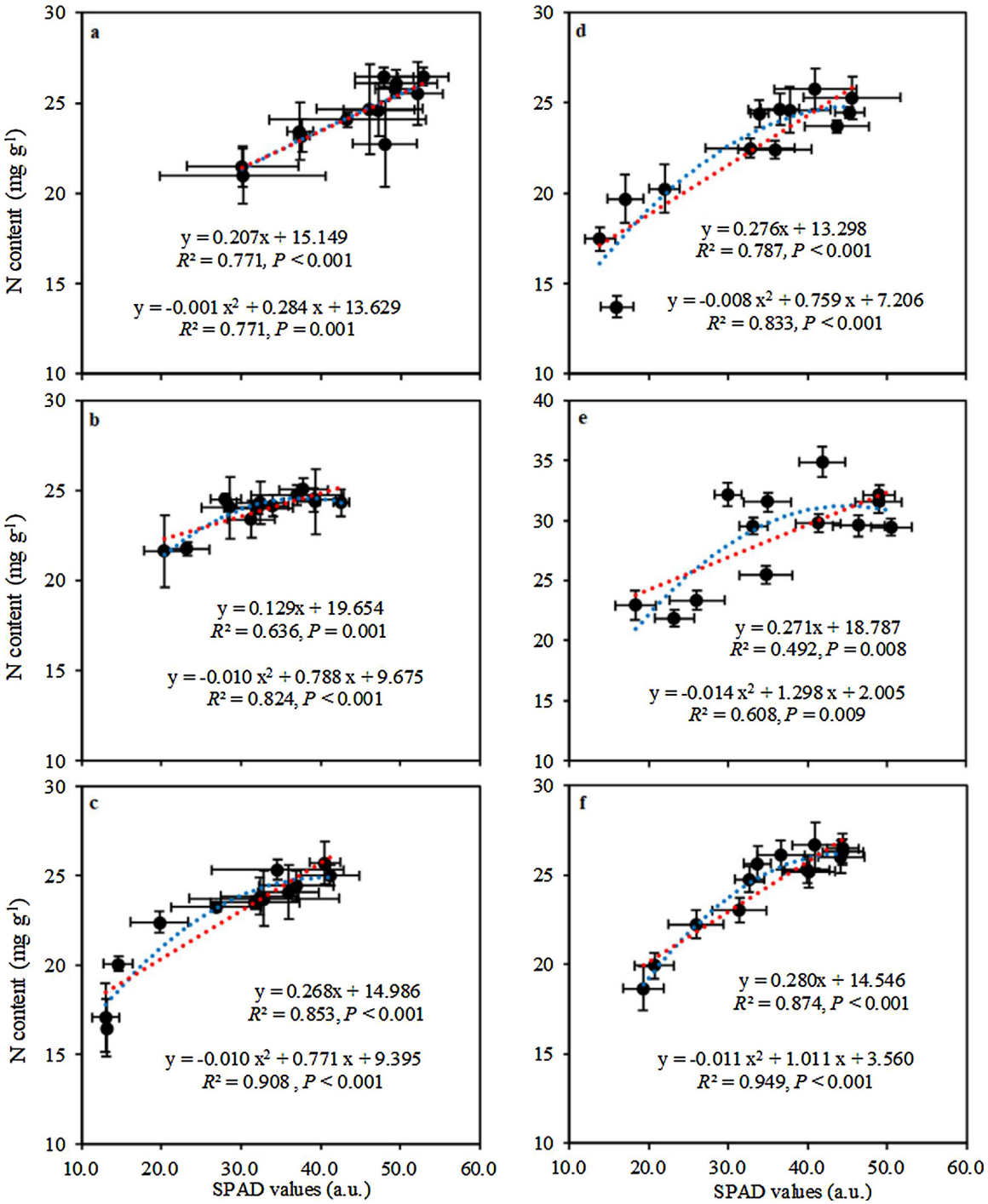

Fig. 8. Relationships between chlorophyll (SPAD a.u.) and nitrogen content under watering regimes. Dotted red and blue lines denote the linear and quadratic functions, respectively. **a**: T_1, control, normal irrigation; **b**: T_2, withholding water during jointing-tasseling; **c**: T_3, jointing-anthesis; **c**: T_4, tasseling-milking; **e**: T_5, silking-milking. They received 260, 188, 138, 136, and 161 mm total irrigation during the whole plant growth period, respectively. **f:** Across all the watering treatments (n = 3 for panels a–e; n = 15 for panel f) (For interpretation of the references to colour in this figure legend, the reader is referred to the web version of this article).

that the highest chlorophyll content (Chl) occurred in the middle leaves, i.e., the ear leaf and the leaves near to it (Fig. 2f). Then, the Chl level generally decreased higher or lower from the middle plant height. Our results showed that the middle leaves, particularly the ear leaves, have higher Chl content. Thus, leaves around the ears may intercept more light to increase the photosynthesis rate, consequently further increasing their contribution to the carbohydrates of the entire plant with high light use efficiency. However, the bottom leaves have the lowest Chl content, as an indicator of the leaf senescence, leading to lowest photosynthesis rate even though the light might penetrate more towards the lower leaves. The current consensus on breeding and field management practices is that Chl status should be improved first in the ear leaves; then, Chl degradation should be limited in the upper and lower leaves. This feature would delay leaf senescence and thereby maintain higher photosynthetic activity in the canopy (Kura-Hotta et al., 1987; Hörtensteiner, 2006). In plants with a low Chl level, plant production could be enhanced by improving the canopy assimilation efficiency under the conditions of lower light in the lower canopy (Gu

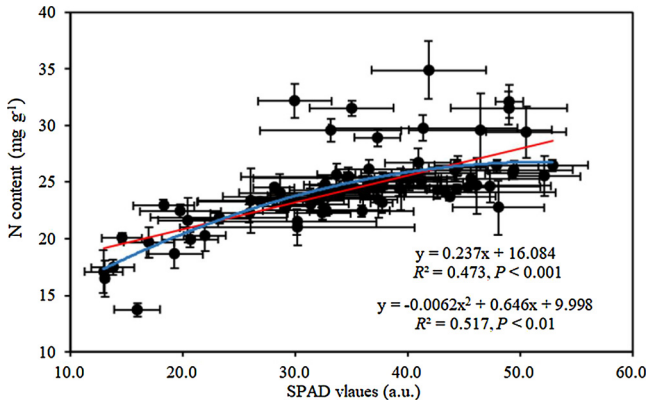

Fig. 9. Relationships between chlorophyll (SPAD a.u.) and nitrogen content across all data (n = 84). Blue and red lines denote the linear and quadratic functional models, respectively (For interpretation of the references to colour in this figure legend, the reader is referred to the web version of this article).

et al., 2017; Walker et al., 2018). This potential for the exploitation of Chl status requires further investigation.

The vertical changes in leaf N content were similar to those of leaf Chl. Specifically, the leaves at the middle plant height had the highest N levels, and these levels subsequently decreased at plant positions above or below the middle level (Fig. 3f). These changes in leaf Chl and N content and LAI along a canopy profile in the field can also be monitored using characteristic spectral signatures by remote sensing methods, including the field-based hyperspectral radiometers' sensor platform (Peng and Gitelson, 2012; Boegh et al., 2013); satellites with remote-sensing-based multispectral sensors, such as MODIS (Moderate Resolution Imaging Spectroradiometer) and SPOT (Satellite for Observation of Earth) (Peng and Gitelson, 2012; Boegh et al., 2013); and unmanned aircraft systems (UAS) (Li et al., 2018). Therefore, remote sensing may be a feasible strategy for evaluating breeding and field management practices when considering functional trait distributions, such as Chl and N content within a crop canopy. Particularly, remote sensing is a nondestructive measurement in precision farming that can feasibly estimate Chl and/or N content (Haboudane et al., 2002; Peng and Gitelson, 2012; Boegh et al., 2013; Delloye et al., 2018). Indeed, the ear leaves and those nearby may contribute the majority of carbohydrates to the ear biomass and may therefore regulate grain yield. However, Chen et al. (2015) indicated that the upper leaves, rather than the ear leaves, had the highest N levels and photosynthetic rates (see also Drouet and Bonhomme, 1999, 2004), suggesting that the Chl and N distributive patterns may depend on the cultivar, planting density, soil nutrition, and watering and fertilizing management (Drouet and Bonhomme, 1999, 2004; Chen et al., 2015; Song et al., 2018; Parajuli et al., 2018).

Many eco-physiological processes affect N metabolism (Kant et al., 2011; Vitale et al., 2011; Sardans and Peñuelas, 2012; Xu et al., 2016). In the present study, rewatering after an episodic drought was expected to trigger some key biological activities, such as N absorption, anabolic N process, photosynthetic capacity, and even plant growth (Xu et al., 2009, 2010; Menezes-Silva et al., 2017; Wang et al., 2017). The optimization of N distribution in a plant under water stress may be achieved by maintaining or even increasing the leaf N content (Farquhar et al., 2002). In the present experiment, the change in vertical N patterns under the T_5 treatment, in which the plants were subjected to drought stress during silking-milking, indicated a higher N level in the middle canopy layers but no change in the total N in the entire canopy (Fig. 3e, Fig. 7d). This result implied that N redistribution rather than increased total canopy N is potentially promoted upon rewatering following water stress. The drought stress is more severe under drought treatment (T_4) at the tasseling-milking stage (drying for 41 days) compared with drought treatment (T_5) at the silking-milking stage (drying for 34 days). Thus, a more severe drought led to a lower leaf N content (Mae, 1997; Xu and Zhou, 2006) under drought stress at the tasseling-milking stage. N reallocation may also lead to different N levels in different organs under different watering treatments at different growth stages (Xu et al., 2006). This finding needs to be studied further.

A linear or power relationship has often been observed between leaf N content and PPFD (e.g., Hirose and Werger, 1987; Drouet and Bonhomme, 1999; Rousseaux et al., 1999; Rorie et al., 2011; Prieto et al., 2012; Pao et al., 2018), and the extent of this relationship depends on the cultivar, planting density, and watering and fertilizing management (Drouet and Bonhomme, 1999, 2004; Prieto et al., 2012; Chen et al., 2015). In addition to light conditions, other environmental factors, such as soil N availability, contribute to the vertical distribution of leaf N (Hirose and Werger, 1987; Anten et al., 1995; Chen et al., 2015). For instance, under high N and ample water conditions, more N is available for redistribution, resulting in a greater N content in the upper layer (Hirose and Werger, 1987; Hikosaka et al., 2016). Gravity and the long pathways involved in water transport could restrict water transport to the upper leaves, and this greater hydraulic limit in the upper leaves could cause the optimal N distribution to be centered in leaves in lower positions (Peltoniemi et al., 2012; Buckley et al., 2013). Our current results showed that the vertical N distribution along a plant in a maize canopy had a unimodal curve pattern. The highest N content occurred in the middle leaves (often the three ear leaves) followed by the upper or lower leaves; this pattern was also affected by drought and subsequent rewatering (Fig. 3).

Simultaneous improvements in productivity and water use might be obtained through crop structural modifications (Drewry et al., 2014). Estimates of the LAIc from the top of the maize plant canopy against the Chl or N gradients showed a quadratic function (Fig. 4) rather than an exponential function (e.g., Anten et al., 1995; Hikosaka et al., 2016). The LAI accounts for most of the variation in gross primary production during the vegetative stage, implying that the amount of leaf area available for light interception could determine plant productivity (Vitale et al., 2016). Our findings on the quadratic functions imply that the exponential functions would be rejected, thereby providing important new information on the patterns of vertical changes in leaf functional traits within a crop canopy. Indeed, the within-canopy gradients of leaf Chl and N could be affected by multiple environmental and plant factors, such as stomatal limitation (Niinemets et al., 2004), altered N source/sink ratios (Uhart and Andrade, 1995; Ciampitti and Vyn, 2013), and N reallocation (Pons et al., 1989; Ciampitti and Vyn, 2013). In particular, maize species/cultivars with the highest maximum photosynthetic capacity often exhibit a less steep N distribution (Hikosaka et al., 2016). Hikosaka et al. (2016) also indicated that the optimal N distribution in maize and rice plant canopies is matched by the light distribution only under conditions of high hydraulic conductance. The results from the present study indicated that a drought and subsequent rewatering treatment may affect the vertical distribution of leaf functional traits, such as N, Chl, and photosynthetic activities (Fig. 4–6). These findings may provide a better understanding of how climate change might affect the optimal patterns of nutrient distribution in an entire canopy.

The positive linear function observed between the Chl and N levels has been reported in many plant species (e.g., Chang and Robison, 2003); in fact, the changes in Chl have been suggested to estimate the leaf N status. For instance, Chang and Robison (2003) found a positive linear functional relationship between foliar N concentration and SPAD meter values in hardwood species, and they suggested that the SPAD-502 chlorophyll meter could be used to obtain a nondestructive and rapid estimation of foliar N status. Nevertheless, other reports have also indicated strong quadratic functions between Chl and N levels (e.g., Wood et al., 1992; Dwyer et al., 1995). Our findings confirmed a good fit for both positive linear functions and quadratic functions for the relationships between the Chl and N levels (Figs. 8 and 9). Moreover, our results also highlighted that the relationships between the Chl and

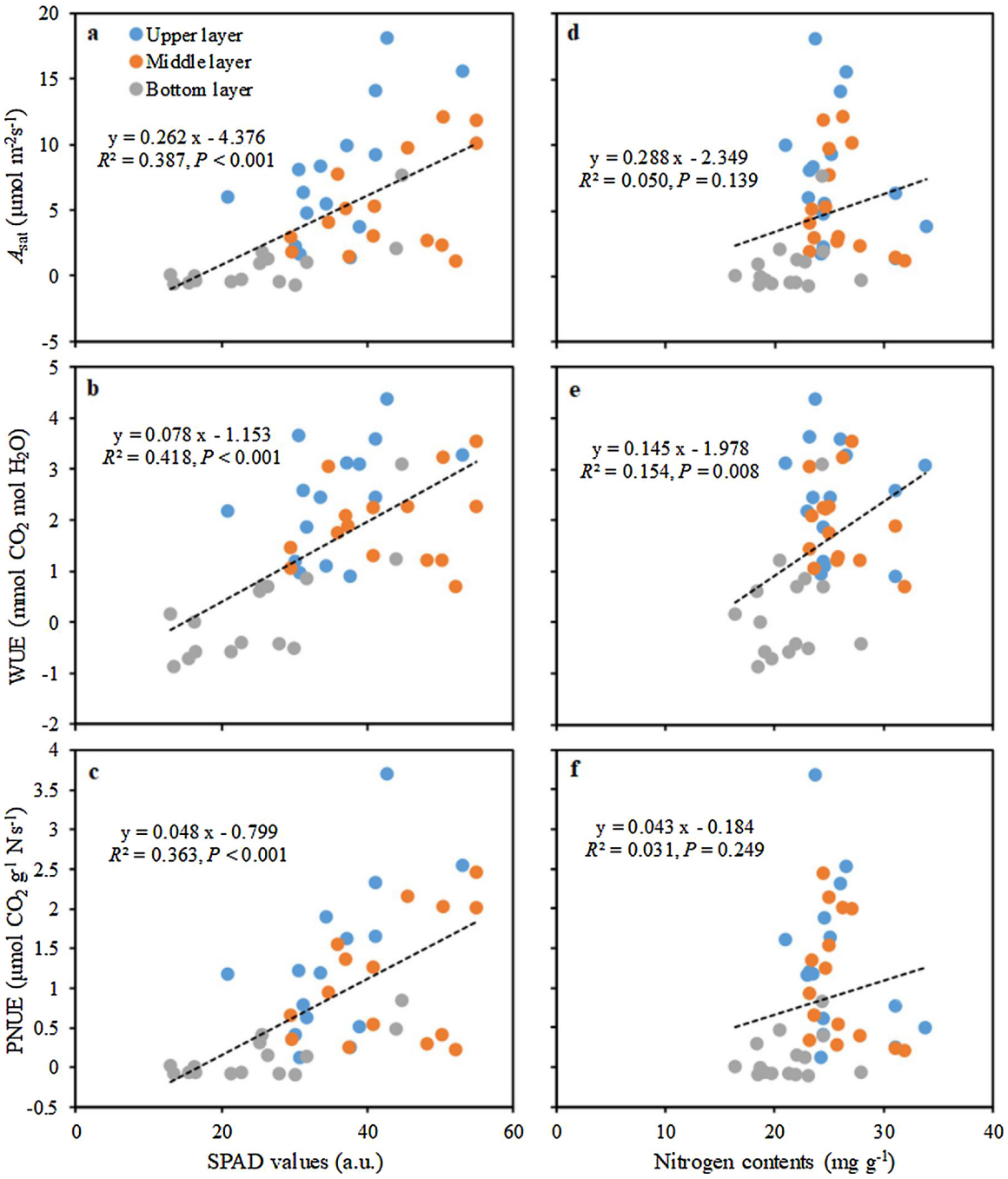

Fig. 10. Associations of net light-saturated photosynthetic rate (A_{sat}, a), water use efficiency (WUE, b), and photosynthetic nitrogen-use efficiency (PNUE, c) with chlorophyll (SPAD a.u., a–c) and nitrogen content (d–f) (n = 45).

N levels can be modified by watering regimes (Fig. 8). Drought conditions increased the slopes of the linear equations but narrowed the parabolic opening of the quadratic functions. Thus, the patterns of the relationships between the Chl and N levels may be equally important indicators of plant responses to water status. Generally, when plant N or Chl levels are relatively low, a better and stronger association may be easily found, depending on the developmental stage, species, and abiotic factors (e.g., Wood et al., 1992; Dwyer et al., 1995; Chang and Robison, 2003; Dunn et al., 2018).

Positive coordinative associations of Chl and N content with A_{sat}, g_s, E, WUE, and PNUE were also indicated by PCA, but negative correlations were observed with C_i, F_v'/F_m', Φ_{PSII}, q_P, and LRI (Fig. 11). Vitale et al. (2007), (2009) also found correlations for g_s with leaf and canopy gas exchange and photosynthetic parameters in response to water status. Comparisons with gas exchange parameters revealed stable responses of the Chl fluorescence parameters to water deficits and leaf aging (Havaux, 1992; Lu and Zhang, 1999; Song et al., 2018). Escobar-Gutiérrez and Combe (2012) indicated that a decrease in Chl content was not concomitant with a dramatic decrease in the fluorescence parameters in maize leaves. Moreover, under environmental stresses, the relationships of growth or grain yield with the functional traits perform differently, depending on growth stages, stress factors, and crop species/cultivars (e.g., Levi et al., 2009; Parajuli et al., 2018; Xu et al., 2018). In addition, the distribution patterns of the PC scores depicted the effects of watering regimes with different canopy layers. This finding highlighted the potential usefulness of PCA for displaying the patterns of the functional responses to watering regimes and the interactions of these watering regimes with leaf senescence.

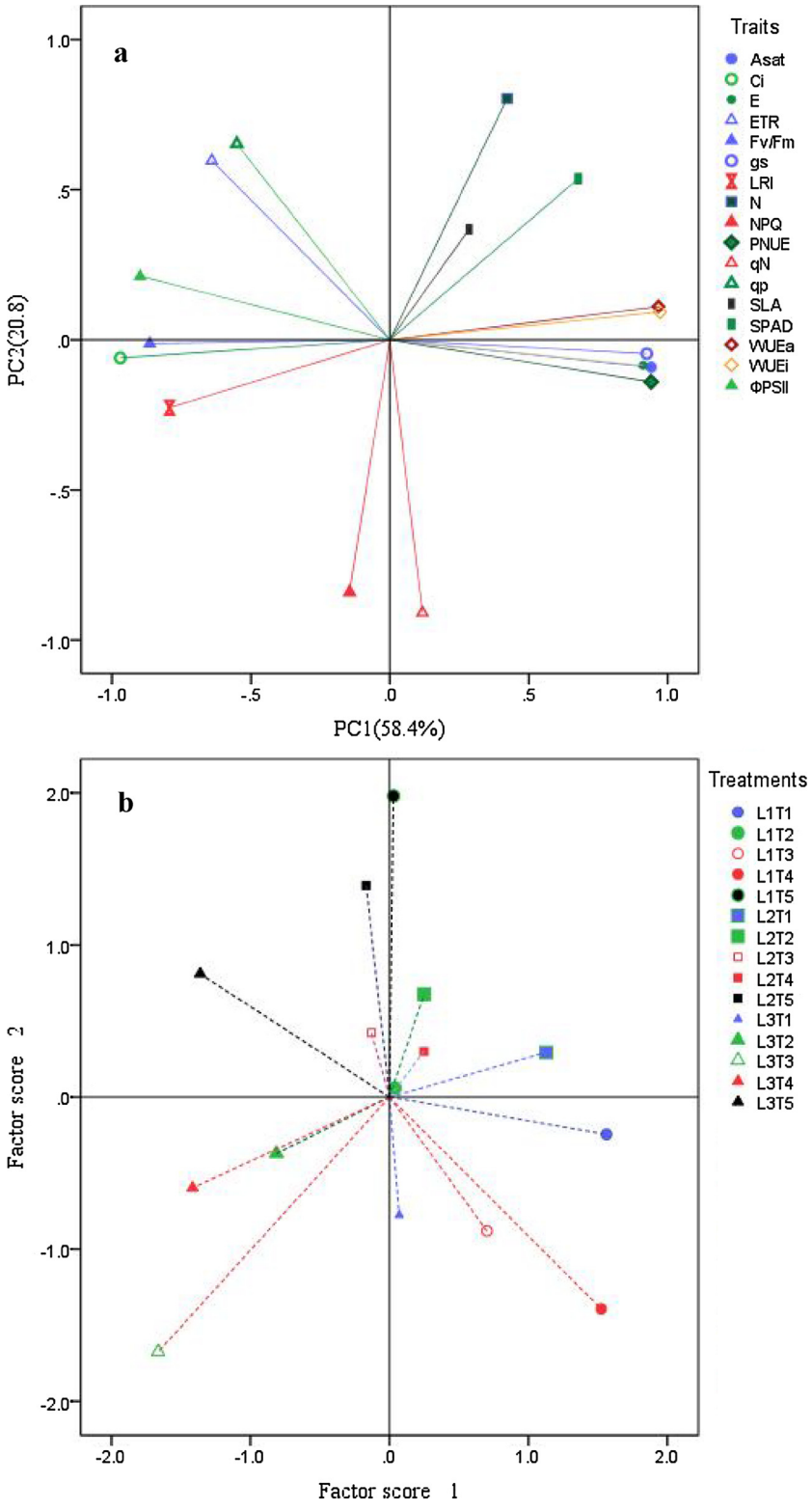

Fig. 11. Principal component analysis (PCA) of leaf functional traits under various precipitation patterns at the three canopy layers, including the traits' loadings (a) and the effect patterns (b). L_1, L_2, and L_3 denote the upper, middle, and bottom layers of the maize plant canopy. T_1, T_2, T_3, T_4, and T_5 represent the normal irrigation and withholding water during jointing-tasseling, jointing-anthesis, tasseling-milking, and silking-milking, respectively. They obtained 260, 188, 138, 136, and 161 mm total irrigation during the whole plant growth period, respectively. Measured on 28, August, 2016, Jinzhou, Liaoning, China. SPAD, relative leaf chlorophyll content (SPAD values, a.u.); N_{mass}, nitrogen content on mass basis; SLA, specific leaf area; A_{sat}, light-saturated photosynthetic rate; g_s, conductance; C_i, intercellular CO_2 concentration; E, transpiration rate; WUE water-use efficiency (A_{sat}/E); WUEi, intrinsic water-use efficiency(A_{sat}/g_s); PNUE, photosynthetic nitrogen use efficiency; F_v'/F_m', photosystem II (PSII) maximum photochemical efficiency; Φ_{PSII}, actual PSII efficiency; q_P, photochemical quenching coefficient; q_N, non-photochemical quenching coefficient; NPQ, non-photochemical quenching coefficient (another form); ETR, electron transport rate; LRI, leaf-rolling index).

5. Conclusions

The present study indicated that the relationship between leaf Chl and N content and LAIc was significantly quadratic rather than exponential. The increased Chl and N distribution in middle leaves within the canopy rather than the top leaves highlights the importance of improving the nutritional status and physiological function of the middle leaves. However, the trajectories of the canopy vertical Chl and N distribution can be modified by drought and rewatering regimes to track the response of photosynthetic activity. Moreover, periodic drought and rewatering appeared to increase the sensitivity of the leaf N content to changes in the Chl level, implying that the association between the Chl and N content could indicate an effect of drought periods. However, the promotion of crop productivity via improving the vertical distribution of the functional traits and their associations within a canopy might depend on crop species, cultivars, local

management practices, local climate and other environmental factors. This information must be investigated further. Nevertheless, our findings may provide new insights into how leaf functional traits are vertically distributed within an entire canopy and how plants will respond to climate change events, such as altered precipitation patterns. These insights could be helpful in plant cultivation for drought resistance and in cultivar selection. This information can be extended to other staple crops, such as wheat and rice, to deeply understand the drought and rewatering process to lay a foundation for establishing effective drought-resistant strategies. This study may also provide data support for the crop modelers to simulate drought effect assessments. In particular, the relationship between Chl and/or N content and LAIc, which could be linked to watering regimes, can been assessed non-destructively by remote sensing methods. This information offers potential for the improved precision management of crops.

Acknowledgements

The study was funded by the China Special Fund for Meteorological Research in the Public Interest (GYHY201506019; GYHY201506001-3), and the National Natural Science Foundation of China (41330531;31661143028). The authors are grateful to Na Mi, Fu Cai, Kunqiao Shi, Yang Yang, and Quanhui Ma for their work during the experiment.

Appendix A. Supplementary data

Supplementary material related to this article can be found, in the online version, at doi:https://doi.org/10.1016/j.agrformet.2019.03.026.

References

Adachi, S., Yoshikawa, K., Yamanouchi, U., Tanabata, T., Sun, J., Ookawa, T., et al., 2017. Fine mapping of carbon assimilation rate 8, a quantitative trait locus for flag leaf nitrogen content, stomatal conductance and photosynthesis in rice. Front. Plant Sci. 8, 60.

Anten, N.P.R., Schieving, F., Werger, M.J.A., 1995. Patterns of light and nitrogen distribution in relation to whole canopy carbon gain in C_3, and C_4, mono-and dicotyledonous species. Oecologia 101, 504–513.

Arunyanark, A., Jogloy, S., Akkasaeng, C., Vorasoot, N., Kesmala, T., Nageswara, R.R.C., et al., 2008. Chlorophyll stability is an indicator of drought tolerance in peanut. J. Agron. Crop Sci. 194, 113–125.

Ata-Ul-Karim, S.T., Zhu, Y., Cao, Q., Rehmani, M., Cao, W., Tang, L., et al., 2017. In-season assessment of grain protein and amylose content in rice using critical nitrogen dilution curve. Eur. J. Agron. 90, 139–151.

Ben-Ari, T., Adrian, J., Klein, T., Calanca, P., Van der Velde, M., Makowski, D., 2016. Identifying indicators for extreme wheat and maize yield losses. Agric. For. Meteorol. 220, 130–140.

Blackmer, T.M., Schepers, J.S., 1995. Use of a chlorophyll meter to monitor nitrogen status and schedule fertigation for corn. J. Prod. Agr. 8, 56–60.

Boegh, E., Houborg, R., Bienkowski, J., Braban, C.F., Dalgaard, T., Van, D.D.T., 2013. Remote sensing of LAI, chlorophyll and leaf nitrogen pools of crop-and grasslands in five European landscapes. Biogeosciences 10, 6279–6307.

Boyer, J.S., 1982. Plant productivity and environment. Science 218, 443–448.

Buckley, T.N., Cescatti, A., Farquhar, G.D., 2013. What does optimization theory actually predict about crown profiles of photosynthetic capacity when models incorporate greater realism? Plant Cell Environ. 36, 1547–1563.

Cattivelli, L., Rizza, F., Badeck, F.W., Mazzucotelli, E., Mastrangelo, A.M., Francia, E., et al., 2008. Drought tolerance improvement in crop plants: an integrated view from breeding to genomics. Field Crop Res. 105, 1–14.

Chang, S.X., Robison, D.J., 2003. Nondestructive and rapid estimation of hardwood foliar nitrogen status using the SPAD-502 chlorophyll meter. Forest Ecol. Manage. 181, 331–338.

Chaves, M.M., Maroco, J.P., Pereira, J.S., 2003. Understanding plant responses to drought—from genes to the whole plant. Funct. Plant Biol. 30, 239–264.

Chen, Y., Wu, D., Mu, X., Xiao, C., Chen, F., Yuan, L., et al., 2015. Vertical distribution of photosynthetic nitrogen use efficiency and its response to nitrogen in field-grown maize. Crop Sci. 56, 397–407.

Ciampitti, I.A., Vyn, T.J., 2013. Grain nitrogen source changes over time in maize: a review. Crop Sci. 53, 366–377.

Delloye, C., Weiss, M., Defourny, P., 2018. Retrieval of the canopy chlorophyll content from Sentinel-2 spectral bands to estimate nitrogen uptake in intensive winter wheat cropping systems. Remote Sens. Environ. 216, 245–261.

Dordas, C.A., 2017. Chlorophyll meter readings, N leaf concentration and their relationship with N use efficiency in oregano. J. Plant Nutr. 40, 391–403.

Drewry, D.T., Kumar, P., Long, S.P., 2014. Simultaneous improvement in productivity, water use, and albedo through crop structural modification. Glob. Change Biol. 20, 1955–1967.

Drouet, J.L., Bonhomme, R., 1999. Do variations in local leaf irradiance explain changes to leaf nitrogen within row maize canopies? Ann. Bot. 84, 61–69.

Drouet, J.M., Bonhomme, R., 2004. Effect of 3D nitrogen, dry mass per area and local irradiance on canopy photosynthesis within leaves of contrasted heterogeneous maize crops. Ann. Bot. 93, 699–710.

Dunn, B.L., Singh, H., Goad, C., 2018. Relationship between chlorophyll meter readings and nitrogen in poinsettia leaves. J. Plant Nutr. 41, 1566–1575.

Dwyer, L.M., Stewart, D.W., 1986. Effect of leaf age and position on net photosynthetic rates in maize (Zea mays L.). Agric. For. Meteorol. 37, 29–46.

Dwyer, L.M., Stewart, D.W., Gregorich, E., Anderson, A.M., Ma, B.L., Tollenaar, M., 1995. Quantifying the nonlinearity in chlorophyll meter response to corn leaf nitrogen concentration. Can. J. Plant Sci. 75, 179–182.

Eapen, D., Martínez-Guadarrama, J., Hernández-Bruno, O., Flores, L., Nieto-Sotelo, J., Cassab, G.I., 2017. Synergy between root hydrotropic response and root biomass in maize (*Zea mays* L.) enhances drought avoidance. Plant Sci. 265, 87–99.

Earl, H.J., Tollenaar, M., 1997. Maize leaf absorptance of photosynthetically active radiation and its estimation using a chlorophyll meter. Crop Sci. 37, 436–440.

Edwards, G.E., Baker, N.R., 1993. Can CO_2 assimilation in maize leaves be predicted accurately from chlorophyll fluorescence analysis? Photosynth. Res. 37, 89–102.

Escobar-Gutiérrez, A.J., Combe, L., 2012. Senescence in field-grown maize: from flowering to harvest. Field Crop Res. 134, 47–58.

Evans, J.R., 1983. Nitrogen and photosynthesis in the flag leaf of wheat (*Triticum aestivum* L.). Plant Physiol. 72, 297–302.

FAO, 2019. Faostat. . Verified, 3 Mar 2019. http://www.fao.org/faostat/en/#data.

Farquhar, G.D., Buckley, T.N., Miller, J.M., 2002. Optimal stomatal control in relation to leaf area and nitrogen content. Silva Fenn. 36, 625–637.

Francis, C.A., Rutger, J.N., Palmer, A.F.E., 1969. A Rapid method for plant leaf area estimation in maize (*Zea mays* L.). Crop Sci. 9, 537–539.

Genty, B., Briantais, J.M., Baker, N.R., 1989. The relationship between the quantum yield of photosynthetic electron transport and quenching of chlorophyll fluorescence. BBA-Gen. Subjects 990, 87–92.

Gray, S.B., Dermody, O., Klein, S.P., Locke, A.M., McGrath, J.M., Paul, R.E., et al., 2016. Intensifying drought eliminates the expected benefits of elevated carbon dioxide for soybean. Nat. Plants 2, 16132.

Greenwood, D.J., Neeteson, J.J., Draycott, A., 1986. Quantitative relationships for the dependence of growth rate of arable crops on their nitrogen content, dry weight and aerial environment. Plant Soil 91, 281–301.

Gu, J., Zhou, Z., Li, Z., Chen, Y., Wang, Z., Zhang, H., et al., 2017. Photosynthetic properties and potentials for improvement of photosynthesis in pale green leaf rice under high light conditions. Front. Plant Sci. 8, 1082.

Guanter, L., Zhang, Y., Jung, M., Joiner, J., Voigt, M., Berry, J.A., et al., 2014. Global and time-resolved monitoring of crop photosynthesis with chlorophyll fluorescence. Proc. Natl. Acad. Sci. U. S. A. 111, E1327–E1333.

Haboudane, D., Miller, J.R., Tremblay, N., Zarco-Tejada, P.J., Dextraze, L., 2002. Integrated narrow-band vegetation indices for prediction of crop chlorophyll content for application to precision agriculture. Remote Sens. Environ. 81, 416–426.

Havaux, M., 1992. Stress tolerance of photosystem II in vivo: antagonistic effects of water, heat and photoinhibition stress. Plant Physiol. 100, 424–432.

Hikosaka, K., Anten, N.P., Borjigidai, A., Kamiyama, C., Sakai, H., Hasegawa, T., et al., 2016. A meta-analysis of leaf nitrogen distribution within plant canopies. Ann. Bot. 118, 239–247.

Hirose, T., Werger, M.J.A., 1987. Maximizing daily canopy photosynthesis with respect to the leaf nitrogen allocation pattern in the canopy. Oecologia 72, 520–526.

Hörtensteiner, S., 2006. Chlorophyll degradation during senescence. Annu. Rev. Plant Physiol. 57, 55–77.

Houles, V., Guerif, M., Mary, B., 2007. Elaboration of a nitrogen nutrition indicator for winter wheat based on leaf area index and chlorophyll content for making nitrogen recommendations. Eur. J. Agron. 27, 1–11.

IPCC, et al., 2014. In: Field, C.B., Barros, V.R., Dokken, D.J., Mach, K.J., Mastrandrea, M.D. (Eds.), Climate Change 2014: Impacts, Adaptation, and Vulnerability. Part A: Global and Sectoral Aspects. Contribution of Working Group II to the Fifth Assessment Report of the Intergovernmental Panel on Climate Change. Cambridge University Press, Cambridge, United Kingdom and New York, NY, USA.

Jin, Z., Zhuang, Q., Wang, J., Archontoulis, S.V., Zobel, Z., Kotamarthi, V.R., 2017. The combined and separate impacts of climate extremes on the current and future us rainfed maize and soybean production under elevated CO_2. Glob. Change Biol. 23, 2687–2704.

Juh, E., Vierling, L.A., Long, D.S., Hunt, E.R., 2011. Early season remote sensing of wheat nitrogen status using a green scanning laser. Agric. For. Meteorol. 151, 1338–1345.

Kant, S., Bi, Y.M., Rothstein, S.J., 2011. Understanding plant response to nitrogen limitation for the improvement of crop nitrogen use efficiency. J. Exp. Bot. 62, 1499–1509.

Kirst, H., Gabilly, S.T., Niyogi, K.K., Lemaux, P.G., Melis, A., 2017. Photosynthetic antenna engineering to improve crop yields. Planta 245, 1009–1020.

Kramer, D.M., Johnson, G., Kiirats, O., Edwards, G.E., 2004. New fluorescence parameters for the determination of QA redox state and excitation energy fluxes. Photosynth. Res. 79, 209–218.

Kura-Hotta, M., Satoh, K., Katoh, S., 1987. Relationship between photosynthesis and chlorophyll content during leaf senescence of rice seedlings. Plant Cell Physiol. 28, 1321–1329.

Levi, A., Ovnat, L., Paterson, A.H., Saranga, Y., 2009. Photosynthesis of cotton near-isogenic lines introgressed with QTLs for productivity and drought related traits.

Plant Sci. 177, 88–96.
Li, R.H., Guo, P.G., Baum, M., Grando, S., Cecarelli, S., 2006. Evaluation of chlorophyll content and fluorescence parameters as indicators of drought tolerance in barley. J. Integr. Agr. 5, 751–775.
Li, J., Shi, Y., Veeranampalayam-Sivakumar, A.N., Schachtman, D.P., 2018. Elucidating sorghum biomass, nitrogen and chlorophyll contents with spectral and morphological traits derived from unmanned aircraft system. Front. Plant Sci. 9, 1406.
Lobell, D.B., Roberts, M.J., Schlenker, W., Braun, N., Little, B.B., Rejesus, R.M., Hammer, G.L., 2014. Greater sensitivity to drought accompanies maize yield increase in the US Midwest. Science 344, 516–519.
Long, S.P., Marshallcolon, A., Zhu, X.G., 2015. Meeting the global food demand of the future by engineering crop photosynthesis and yield potential. Cell 161, 56–66.
Lu, C., Zhang, J., 1999. Effects of water stress on photosystem II photochemistry and its thermostability in wheat plants. J. Exp. Bot. 50, 1199–1206.
Mae, T., 1997. Physiological nitrogen efficiency in rice: nitrogen utilization, photosynthesis, and yield potential. Plant Soil 196, 201–210.
Makino, A., Osmond, B., 1991. Solubilization of ribulose-1,5-bisphosphate carboxylase from the membrane fraction of pea leaves. Photosynth. Res. 29, 79–85.
Maxwell, K., Johnson, G.N., 2000. Chlorophyll fluorescence—a practical guide. J. Exp. Bot. 51, 659–668.
Menezes-Silva, P.E., Sanglard, L.M., Ávila, R.T., Morais, L.E., Martins, S.C., Nobres, P., et al., 2017. Photosynthetic and metabolic acclimation to repeated drought events play key roles in drought tolerance in coffee. J. Exp. Bot. 68, 4309–4322.
Meng, Q., Hou, P., Wu, L., Chen, X., Cui, Z., Zhang, F., 2013. Understanding production potentials and yield gaps in intensive maize production in China. Field Crop Res. 143, 91–97.
Muryono, M., Chen, C.P., Sakai, H., Tokida, T., Hasegawa, T., Usui, Y., et al., 2017. Nitrogen distribution in leaf canopies of high-yielding rice cultivar Takanari. Crop Sci. 57, 2080–2088.
Myers, S.S., Smith, M.R., Guth, S., Golden, C.D., Vaitla, B., Mueller, N.D., et al., 2017. Climate change and global food systems: potential impacts on food security and undernutrition. Annu. Rev. Publ. Heal. 38, 259–277.
Nakabayashi, R., Yonekura-Sakakibara, K., Urano, K., Suzuki, M., Yamada, Y., Nishizawa, T., et al., 2014. Enhancement of oxidative and drought tolerance in *Arabidopsis* by overaccumulation of antioxidant flavonoids. Plant J. 77, 367–379.
Niinemets, Ü., Sonninen, E., Tobias, M., 2004. Canopy gradients in leaf intercellular CO_2, mole fractions revisited: interactions between leaf irradiance and water stress need consideration. Plant Cell Environ. 27, 569–583.
Pao, Y.C., Chen, T.W., Pascal Moualeu-Ngangue, D., Stützel, H., 2018. Environmental triggers for photosynthetic protein turnover determine the optimal nitrogen distribution and partitioning in the canopy. J. Exp. Bot. https://doi.org/10.1093/jxb/ery308.
Parajuli, S., Ojha, B.R., Ferrara, G.O., 2018. Quantification of secondary traits for drought and low nitrogen stress tolerance in inbreds and hybrids of maize (*Zea mays* L.). J. Plant Genet. Breed. 2, 106.
Peltoniemi, M.S., Duursma, R.A., Medlyn, B.E., 2012. Co-optimal distribution of leaf nitrogen and hydraulic conductance in plant canopies. Tree Physiol. 32, 510–519.
Peng, Y., Gitelson, A.A., 2012. Remote estimation of gross primary productivity in soybean and maize based on total crop chlorophyll content. Remote Sens. Environ. 117, 440–448.
Pons, T.L., Schieving, F., Hirose, T., Werger, M.J.A., 1989. Optimization of Leaf Nitrogen Allocation for Canopy Photosynthesis in *Lysimachia vulgaris*. Causes and Consequences of Variation in Growth Rate and Productivity of Higher Plants. SPB Academic, The Hague, pp. 175–186.
Prieto, J.A., Louarn, G., Perez, Pena J., Ojeda, H., Simonneau, T., Lebon, E., 2012. A leaf gas exchange model that accounts for intra-canopy variability by considering leaf nitrogen content and local acclimation to radiation in grapevine (*Vitis vinifera* L.). Plant Cell Environ. 35, 1313–1328.
Rorie, R.L., Purcell, L.C., Mozaffari, M., Karcher, D.E., King, C.A., Marsh, M.C., Longer, D.E., 2011. Association of "greenness" in corn with yield and leaf nitrogen concentration. Agron. J. 103, 529–535.
Rousseaux, M.C., Hall, A.J., Sanchez, R.A., 1999. Light environment, nitrogen content, and carbon balance of basal leaves of sunflower canopies. Crop Sci. 39, 1093–1100.
Ruiz-Sánchez, M.C., Domingo, R., Torrecillas, A., Pérez-Pastor, A., 2000. Water stress preconditioning to improve drought resistance in young apricot plants. Plant Sci. 156, 245–251.
Sardans, J., Peñuelas, J., 2012. The role of plants in the effects of global change on nutrient availability and stoichiometry in the plant-soil system. Plant Physiol. 160, 1741–1761.
Schepers, J.S., Francis, D.D., Vigil, M., Below, F.E., 1992. Comparison of corn leaf nitrogen concentration and chlorophyll meter readings. Commun. Soil Sci. Plant Anal. 23, 2173–2187.
Schlemmer, M., Gitelson, A., Schepers, J., Ferguson, R., Peng, Y., Shanahan, J., Rundquist, D., 2013. Remote estimation of nitrogen and chlorophyll contents in maize at leaf and canopy levels. INT J. Appl. Earth OBS. 25, 47–54.
Schröder, J.J., Neeteson, J.J., Oenema, O., Struik, P.C., 2000. Does the crop or the soil indicate how to save nitrogen in maize production?: reviewing the state of the art. Field Crop Res. 66, 151–164.
Schulze, E.D., 1986. Carbon dioxide and water vapor exchange in response to drought in the atmosphere and in the soil. Annu. Rev. Plant Biol. 37, 247–274.
Schwantes, A.M., Swenson, J.J., Gonzalez-Roglich, M., Johnson, D.M., Domec, J.C., Jackson, R.B., 2017. Measuring canopy loss and climatic thresholds from an extreme drought along a fivefold precipitation gradient across Texas. Glob. Change Biol. 23, 5120–5135.
Sharp, R.E., Poroyko, V., Hejlek, L.G., Spollen, W.G., Springer, G.K., Bohnert, H.J., et al., 2004. Root growth maintenance during water deficits: physiology to functional genomics. J. Exp. Bot. 55, 2343–2351.
Sinclair, T.R., Horie, T., 1989. Leaf nitrogen, photosynthesis, and crop radiation use efficiency: a review. Crop Sci. 29, 90–98.
Song, H., Li, Y.B., Zhou, L., Xu, Z.Z., Zhou, G.S., 2018. Maize leaf functional responses to drought episode and rewatering. Agric. For. Meteorol. 249, 57–70.
Trenberth, K.E., Dai, A., Van Der Schrier, G., Jones, P.D., Barichivich, J., Briffa, K.R., Sheffield, J., 2014. Global warming and changes in drought. Nat. Clim. Change 4, 17–22.
Uhart, S.A., Andrade, F.H., 1995. Nitrogen and carbon accumulation and remobilization during grain filling in maize under different source/sink ratios. Crop Sci. 35, 183–190.
Vitale, L., Tommasi, P.D., Arena, C., Fierro, A., Santo, A.V.D., Magliulo, V., 2007. Effects of water stress on gas exchange of field grown *Zea mays* L. In southern Italy: an analysis at canopy and leaf level. Acta Physiol. Plant. 29, 317–326.
Vitale, L., Tommasi, P.D., Arena, C., Riondino, M., Forte, A., Verlotta, A., et al., 2009. Growth and gas exchange response to water shortage of a maize crop on different soil types. Acta Physiol. Plant. 31, 331–341.
Vitale, L., Arena, C., Carillo, P., Di Tommasi, P., Mesolella, B., Nacca, F., et al., 2011. Gas exchange and leaf metabolism of irrigated maize at different growth stages. Plant Biosyst. 145, 485–494.
Vitale, L., Tommasi, P.D., D'Urso, Guido, Magliulo, V., 2016. The response of ecosystem carbon fluxes to LAI and environmental drivers in a maize crop grown in two contrasting seasons. Int. J. Biometeorol. 60, 411–420.
Walker, B.J., Drewry, D.T., Slattery, R.A., Vanloocke, A., Cho, Y.B., Ort, D.R., 2018. Chlorophyll can be reduced in crop canopies with little penalty to photosynthesis. Plant Physiol. 176, 1215–1232.
Wang, H., Yang, Z., Yu, Y., Chen, S., He, Z., Wang, Y., et al., 2017. Drought enhances nitrogen uptake and assimilation in maize roots. Agron. J. 109, 39–46.
Wood, C.W., Reeves, D.W., Duffield, R.R., Edmisten, K.L., 1992. Field chlorophyll measurements for evaluation of corn nitrogen status. J. Plant Nutr. 15, 487–500.
Xiang, J.J., Zhang, G.H., Qian, Q., Xue, H.W., 2012. Semi-rolled leaf1 encodes a putative glycosylphosphatidylinositol-anchored protein and modulates rice leaf rolling by regulating the formation of bulliform cells. Plant Physiol. 159, 1488–1500.
Xu, Z.Z., Yu, Z.W., Wang, D., 2006. Nitrogen translocation in wheat plants under soil water deficit. Plant Soil 280, 291–303.
Xu, Z.Z., Zhou, G.S., Shimizu, H., 2009. Are plant growth and photosynthesis limited by pre-drought following rewatering in grass? J. Exp. Bot. 60, 3737–3749.
Xu, Z.Z., Zhou, G.S., Shimizu, H., 2010. Plant responses to drought and rewatering. Plant Sign. Behav. 5, 649–654.
Xu, Z.Z., Jiang, Y.L., Zhou, G.S., 2016. Nitrogen cycles in terrestrial ecosystems: climate change impacts and mitigation. Environ. Rev. 24, 132–143.
Xu, Z.Z., Zhou, G.S., Han, G.X., Li, Y.J., 2018. The relationship between leaf and ecosystem CO_2 exchanges in a maize field. Acta Physiol. Plant. 40, 156.
Xu, Z.Z., Zhou, G.S., 2006. Combined effects of water stress and high temperature on photosynthesis, nitrogen metabolism and lipid peroxidation of a perennial grass Leymus chinensis. Planta 224, 1080–1090.
Zhang, R.H., Xue, J.Q., Pu, J., Zhao, B., Zhang, X.H., Zheng, Y.J., Bu, L.D., 2011. Effects of drought stress on plant growth and photosynthetic characteristic of maize seedlings. Acta Agron. Sin. 37, 521–528.
Zhou, B., Sun, X., Ding, Z., Ma, W., Zhao, M., 2017. Multisplit nitrogen application via drip irrigation improves maize grain yield and nitrogen use efficiency. Crop Sci. 57, 1687–1703.